Adsorption Kinetics of a Hydrophobic−Hydrophilic Diblock Polyelectrolyte at the Solid−Aqueous Solution Interface: A Slow Birth and Fast Growth Process

T. Abraham,[†,⊥] S. Giasson,[*,†] J. F. Gohy,[‡] R. Jérôme,[‡] B. Müller,[§] and M. Stamm[*,§]

Department of Chemical Engineering and CERSIM, Laval University, Sainte-Foy, Québec, Canada G1K 7P4; Center for Education and Research on Macromolecules, University of Liège, Sart-Tilman B6, 4000 Liège, Belgium; and Max-Planck-Institut für Polymerforschung, Ackermannweg 10, 55128 Mainz, Germany

Received July 22, 1999; Revised Manuscript Received February 14, 2000

ABSTRACT: The adsorption kinetics of a diblock copolymer poly(*tert*-butyl methacrylate)-*b*-poly(glycidyl methacrylate sodium sulfonate) on hydrophobic substrate from aqueous solution under different added monovalent salt (NaCl) concentrations was investigated using an ellipsometric technique. The effect of monovalent counterion size on adsorption kinetics of the same copolymer on hydrophobic surfaces was also part of the investigation. The results, in general, indicate that the adsorption process on solid surfaces occurs through the anchoring of hydrophobic chains due to the short-ranged hydrophobic interactions. The kinetic data reveal three distinct stages in the adsorption process: an incubation period, a subsequent fast growth process of the polymer layer, and a plateau (equilibrium) region. These three stages are found to be influenced by salt concentration as well as counterion size. The equilibrium adsorption density increases as a function of salt concentration, and the dependence is found to be different from the theoretical predictions. The incubation time increases with salt concentration according to a power law dependence, and a simple bound ionic layer formation on the substrate is proposed as a possible explanation for this observation. An attempt has been made to explain the growth process in terms of an Avrami type ordering process. The Avrami analysis indicates that the buildup of polyelectrolyte layer structure depends on added salt conditions. Our kinetic data suggest that the diffusion of the chains to the surface is not the rate-controlling process for adsorption. A slow birth (nucleation) and fast growth of the layer seem to be the determining adsorption process.

Introduction

The solution and interfacial characteristics of polyelectrolytes have been investigated intensively in the past few years.[1,2] The adsorbed and end-tethered polyelectrolyte structures at interfaces are considered as a model system for a broad spectrum of interfaces ranging from cell surfaces interacting with their surrounding to an increasing number of situations in colloidal technology, for example colloidal stabilization in polar solvents. In such situations the polyelectrolytes or ionic macromolecules are used to modify and control the surface interactions. The most important technological aspect of colloid stabilization with the end-tethered polyelectrolytes is the fact that the interaction is much less sensitive to Debye screening with added electrolytes than simply charged surfaces. A similar end grafting topology can be obtained by adsorbing hydrophobic−hydrophilic block copolymers (macrosurfactants) with the hydrophobic block adsorbing on the surface and the polyelectrolyte block dangling in the solution. The solutions of such diblock polyelectrolytes have been investigated theoretically and experimentally in a great deal.[3−9] However, while adsorption characteristics are explored theoretically to a certain extent,[3,4,10−20] very little is known experimentally about the adsorption kinetics of diblock polyelectrolyte systems at the solid−liquid interface.

The adsorption kinetics and the equilibrium properties of neutral di- and triblock copolymers in nonpolar solvents have been investigated at a considerable level.[21−25] The process of adsorbed layer formation at a solid interface is essentially considered as a two-stage process: (a) an initial fast process during which the polymer chains or aggregates diffuse from solution to bare substrate and thereby a monolayer is formed; (b) a subsequent slow buildup process where the chains penetrate through the existing monolayer in conjunction with conformational rearrangement of the chains. The chain characteristics and therefore the adsorption properties of hydrophobic−hydrophilic diblock polyelectrolytes differ much from those of diblock neutral copolymers due to the electrostatic interactions and screening effect of added salt. Two different types of ionic block can be used: (a) strongly charged ionic block whose charge density is very sensitive to added salt concentrations; (b) weakly charged ionic block whose charge density can be controlled by adjusting the pH. It is generally accepted that the strongly charged polyelectrolyte is highly stretched in dilute solutions with no added salt where electrostatic interactions between the segments determine the backbone conformation by increasing both the effective persistence length of the chain and the excluded volume in solution. Under added salt conditions, the range of electrostatic interactions is reduced due to the screening effects, and the chain begins to lose its stiffness, therefore causing a decrease in the chain persistence length.

There has been considerable experimental investigation on adsorption of homopolyelectrolytes at solid−liquid interfaces,[26,27] but there is not much literature

[†] Laval University.
[‡] University of Liège.
[§] Max-Planck-Institut für Polymerforschung.
* Address correspondence to either of these authors: sgiasson@gch.ulaval.ca or stamm@mpip-mainz.mpg.de.
[⊥] This work forms part of the Ph.D. dissertation of T. Abraham.

10.1021/ma991207j CCC: $19.00
Published on Web 07/22/2000

concerning the adsorption characteristics of hydrophobic−hydrophilic (electrolytic) diblock polyelectrolytes. A relatively close study on that topic is the adsorption kinetics study of diblock polyelectrolyte based on poly(*tert*-butyl polystyrene)-*b*-poly(styrene sodium sulfonate).[28] In this study, a threshold salt concentration for the adsorption of such diblock copolymers on thermally grown silicon oxide surfaces has been observed, and the kinetics is explained in terms of a two-stage process as in the case of neutral diblock copolymers.[21] Recently, there has been a report on adsorption characteristics of ampholytic diblock copolymer on hydrophilic substrate.[29] It has been shown that the adsorbed amount reaches its maximum at the isoelectric point of the polyampholyte. A Fickian diffusion model was used to describe the adsorption kinetics data, and interestingly, the diffusion coefficient of the polyampholyte toward the surface measured in the early stage of adsorption has been shown to be a function of pH and both the polyampholyte and the salt concentrations. This observation is qualitatively in good agreement with the slow diffusion process of polyelectrolytes in solution.

The present study is concerned with the adsorption kinetics of a diblock copolymer of poly(*tert*-butyl methacrylate)-*b*-poly(glycidyl methacrylate sodium sulfonate) to be denoted by (PtBMA-*b*-PGMAS) on hydrophobized silicon substrate from aqueous solution under no added salt and different added salt concentrations. The backbone of the polyelectrolyte block of the PtBMA-*b*-PGMAS molecule is chemically much different from the backbone of poly(styrenesulfonate) since methacrylic group is polar while polystyrene is not. Moreover, glycidyl groups contain a free hydroxyl group which may undergo specific interaction with added counterions (Na^+). Therefore, one could presume that the screening response and the adsorption characteristics of the PtBMA-*b*-PGMAS molecules to added salt are different from that of styrene-based polyelectrolytes. The main objective of this study is to comprehend the surface growth phenomena and the structural properties of strongly charged adsorbed polyelectrolyte layers. This objective was achieved by investigating the effects of monovalent salt (NaCl) concentration and monovalent counterion size on adsorption kinetics of hydrophobic−hydrophilic diblock polyelectrolyte (PtBMA-*b*-PGMAS) on hydrophobic and hydrophilic surfaces using mainly an ellipsometric technique.

Experimental Section

Materials. The chemical structure of the diblock copolymer of poly(*tert*-butyl methacrylate)-*b*-poly(glycidyl methacrylate sodium sulfonate) (PtBMA-*b*-PGMAS) is shown in Figure 1. It was synthesized by the anionic polymerization technique. In a typical polymerization experiment, the glass reactor containing the required amount of LiCl (10/1 LiCl/initiator molar ratio) was flame-dried under vacuum and purged with nitrogen, and then tetrahydrofuran (THF) was added and cooled to 0 °C. Diphenylmethyllithium was added drop by drop until a persistent yellow color was observed, followed by the required amount of initiator. The BMA monomer was then added and polymerized for 30 min. A small sample was withdrawn from the polymerization medium for characterization. The GMA monomer was added at −78 °C and polymerized for 2 h. The living anions left were finally deactivated by a few drops of acidified methanol. PtBMA-*b*-PGMA copolymer was converted into PtBMA-*b*-PGMAS by ring-opening of the oxirane group of GMA promoted by sodium sulfite. Sodium sulfite (50 g) and tetrabutylammonium bromide (transfer

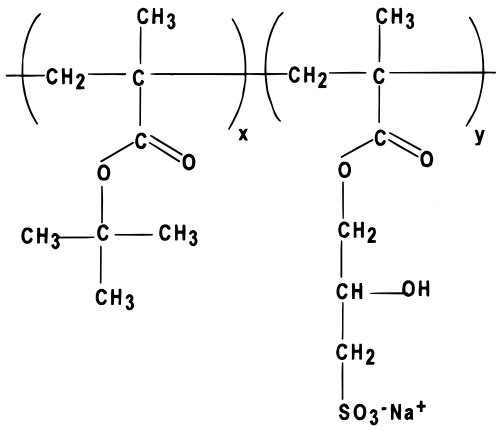

Figure 1. Chemical structure of poly(*tert*-butyl methacrylate)-*b*-sodium poly(glycidyl methacrylate sulfonate) [PtBMA-*b*-PGMAS].

catalyst, 33 g) were dissolved in 200 mL of deionized water in a 1 L flask equipped with a condenser. The finely divided block copolymer (20 g) was suspended in the stirred aqueous solution, and 20 mL of chloroform was finally added. The suspension was deoxygenated with a stream of nitrogen and heated at 80 °C for 30 h. After titration, the yield of sulfonation was calculated to be 78%. The final product was purified by dialysis against distilled water (Spectra-Por membranes, cutoff 10 000 Da).

Molecular weight and molecular weight distribution were determined by size exclusion chromatography (SEC) at 35 °C in THF using a Hewlett-Packard 1050 liquid chromatogram equipped with two PLGel columns (1000 and 10 000) and a Hewlett-Packard 1047A refractive index detector. Poly(methyl methacrylate) standards were used for calibration. For diblock copolymers, the M_n of the second block was determined by ^1H NMR using a Bruker AM400 equipment. Molecular weight characteristics: $M_{n(PtBMA)}$ (g/mol) = 3700; $M_{n(PGMAS)}$ (g/mol) = 23 900; $M_w/M_n = 1.10$. The PtBMA-*b*-PGMAS diblock is a self-associating macrosurfactant. In water solution, the hydrophobic block will form a collapsed core while the hydrophilic block will be solvated with a characteristic coil dimension that will depend on the size of the block and the salt concentration in solution. The critical micelle concentration (cmc) has been determined by surface tension measurement and was found to be approximately 0.02% (w/w). A PGMAS homopolymer of molecular weight (M_n) 22 000 (g/mol) and MWD 1.59 was also used. The homopolymer PGMAS was prepared by radical polymerization of GMA in THF at 50 °C, initiated by azobis(isobutyronitrile) (AIBN). The PGMA homopolymer was then precipitated in methanol and transformed in PGMAS by the same procedure as the one used for the diblock PtBMA−PGMAS.

Silicon wafers were obtained from MEMC Electronic Materials Inc., Spartauburg, with a native oxide layer of thickness 2 nm and were used as substrate for adsorption studies. The silicon wafers were cut into rectangular pieces of dimensions 2.1 × 1.5 cm. The slides were then cleaned with dichloromethane in an ultrasonic bath for 15 min at about 50 °C in order to remove possible organic surface contamination. Afterward, the wafers were rinsed with Milli-pore water. This was followed by an oxidation step in a mixture of H_2O_2, NH_3, and water at about 75 °C for about 30−45 min. After rinsing thoroughly with Milli-pore water, the slides were dried with clean nitrogen. This treatment rendered the surface hydrophilic by generating silanol groups (Si−OH). These hydrophilic surfaces were kept in absolute ethanol until use to maintain its hydrophilic character. Before use, they were rinsed with Milli-pore water and dried with purified nitrogen. Hydrophobic slides were prepared by treating hydrophilic slides with 0.2% (v/v) dichlorodimethylsilane in trichloroethane for 2 h. They were then rinsed several times with trichloroethane and ethanol. Afterward, the surfaces were kept in absolute ethanol.

Prior to use, they were rinsed with Milli-pore water and dried with purified nitrogen.

To ensure the hydrophilic and hydrophobic character of the substrate, contact angle measurements were conducted using a standard microscope. The contact angles for hydrophilic and hydrophobic surfaces were found to be in the range of 13−15° and 85−90°, respectively. A phase interference microscope purchased from LOT/ZYGO was used to characterize the sample surfaces with a lateral resolution of approximately 1 μm and a height resolution of 0.6 nm. The magnification used was 100 times. The principle of operation is described elsewhere.[30] The substrates, both hydrophobic and hydrophilic, were found to be smooth, and the roughness is less than 0.8 nm. The substrates have also been characterized by ellipsometric measurements. The oxide layer thickness (before silane treatment) and the silane layer thickness (after silane treatment) were found to be 1.2 ± 0.2 and 0.6 ± 0.1 nm, respectively. The ellipsometric readings for a given substrate at different locations were found to be very much consistent; therefore, both oxide layer and silane layer can be considered relatively smooth and homogeneous.

Dynamic Light Scattering. To characterize the 100 ppm PtBMA-*b*-PGMAS solution under different salt concentrations, dynamic light scattering measurements were performed using a commercial ALV 3000 digital correlator. The light source used was a 400 mW krypton ion laser of wavelength $\lambda = 647.1$ nm. Autocorrelation functions $g_q(t)$, were measured for solutions at several salt concentrations with 100 ppm PtBMA-*b*-PGMAS solution. The scattering angle was 120°, and the temperature was set to 22 °C. The data analysis was performed using CONTIN, a constrained regularization method program for the inverse Laplace transformation of dynamic light scattering data. The CONTIN program is able to characterize the distribution of relaxation times in the experimental time correlation functions. The hydrodynamic radius R_H of particles and the free particle diffusion coefficient in solution (D_{DLS}) are interrelated by the Stokes−Einstein relation:

$$R_H = kT/6\pi\eta D_{DLS} \tag{1}$$

where k is the Boltzmann constant, T the temperature, and η the viscosity of the solvent.

Ellipsometry. The ellipsometric measurements were performed with home-built computer controlled null ellipsometer in a vertical polarizer−compensator−sample−analyzer (P−C−S−A) arrangement.[21] A He−Ne laser ($\lambda = 632.8$ nm) was used as light source. The angle of incidence was set to 70.0° to obtain the best sensitivity in our experimental conditions. Using a motorized linear polarizer (P) and a compensator (C), a state of elliptical polarization is generated which, after reflection, becomes linear polarized light. The reflected light is extinguished by an analyzer (A), which is in fact a second polarizer. The intensity of reflected light passing through analyzer is detected by the photomultiplier. The computer-controlled polarizer and analyzer allows the automated search for the null settings or minimum intensity. At the null settings, the position of polarizer (P_A^0) gives the ellipsometric angle, Δ, or relative phase difference, ($\Delta = 2P_A^0 + 90$), and the position of the analyzer (A_A^0) gives the ellipsometric angle Ψ ($\Psi = A_A^0$). The Δ and Ψ angles contain information about the relative phase shift and attenuation of the component waves perpendicular (s-wave) and parallel (p-wave) to the plane of incidence, respectively. Thus, both the relative phase difference (Δ) and the amplitude ratio (tan Ψ) corresponding to the change in reflection are obtained from the ellipsometer readings. The ellipsometry technique is well described in the literature.[31]

The adsorption experiments were performed in a specially designed trapezoidal Teflon cell at room temperature and fixed humidity. Initially, the cell containing the substrate rigidly mounted to a Teflon table was filled with an aqueous solution at a desired salt concentration. The ellipsometric angles Ψ and Δ were measured as a function of time to check the stability of the system with and without salt. A pair of ellipsometric angles were recorded at every 23 s. To ensure homogeneity of the system, a small magnetic stirrer was kept under the substrate mounting table for gentle stirring. A known volume of concentrated polymer solution was added in order to obtain a final concentration of 100 ppm solution, and at that time ($t = 0$), the changes in Ψ and Δ were recorded as a function of time. The measurements were conducted until the equilibrium was reached, i.e., until no more change in ellipsometric angles was detected.

Table 1. Refractive Index Increments of Polymer and Salts Used

materials	dn/dc (mL/g)	materials	dn/dc (mL/g)
PtBMA-*b*-PGMAS	0.1440	KCl	0.1352
NaCl	0.1720	RbCl	0.0900
LiCl	0.2033	CsCl	0.0781

Data Analysis. The ellipsometry data were analyzed assuming that the adsorbed polymer molecules form a homogeneous isotropic polymer layer on the silicon wafer. The basic equations of eliipsometry[32] were used to determine the refractive index n_1 and thickness d_1 of the polymer layer. Two different cases have been considered: (i) when the light is reflected directly from the substrate (hydrophobized silicon wafers), the Drude equation[31] is

$$\tan(\Psi)e^{i\Delta} = \frac{r_p}{r_s} = f(n_2,d_2,n_3,d_3,N_4,n_0,\phi_0,\lambda) \tag{2}$$

where r_p and r_s are the complex reflectances for the substrate parallel and perpendicular to the plane of incidence, N_4 is the complex refractive index of the silicon substrate ($N_4 = n_4 + ik$), n_2, n_3, and n_0 are the refractive indexes of the silane layer, the silicon oxide layer, and the surrounding solution, respectively, d_2 and d_3 are the thickness of the silane and silicon oxide layers, respectively, and ϕ_0 is the angle of incidence; and (ii) with a thin polymer film on the substrate (adsorbed copolymer), the Drude equation[31] is

$$\tan(\Psi)e^{i\Delta} = \frac{r_p}{r_s} = f(n_1,d_1,n_2,d_2,n_3,d_3,N_4,n_0,\phi_0,\lambda) \tag{3}$$

where n_1 and d_1 are the refractive index and the thickness of polymer film, respectively. To calculate the refractive index of the solution, one has to take into account the contribution of all solution components (water, copolymer, salt):

$$n_0 = n_{water} + \left(\frac{dn}{dc}\right)_{salt} c_{salt} + \left(\frac{dn}{dc}\right)_{polymer} c_{polymer} \tag{4}$$

where n_{water} is the refractive index of water and $(dn/dc)_x$ is the refractive index increment of species x and c_x is the concentration of species x. Table 1 features the refractive index increments of each species used in this study which were determined with a differential refractometer. Homemade software is used to solve the complex eq 3 in order to obtain refractive index (n_1) and adsorbed layer thickness (d_1) of the polymer from the ellipsometric data (Δ and ψ). The details have been described elsewhere.[21] The adsorbed amount A (mg/m^2) can be calculated using the following equation:[32]

$$A = \frac{d_1(n_1 - n_0)}{(dn/dc)_{polymer}} \tag{5}$$

Since the differences in refractive indices between the polymer and solution are small, the independent determination of n_1 and d_1 is difficult. However, the product n_1d_1 does not depend on the adopted layer model. The adsorbed amount determined according to eq 5 does not depend on the type of concentration profile near the wall: step, parabolic, or exponential.[21]

Results

Adsorption on Hydrophobic Surface. The adsorption data obtained from the adsorption studies of PtBMA-*b*-PGMAS on the hydrophobic surfaces are

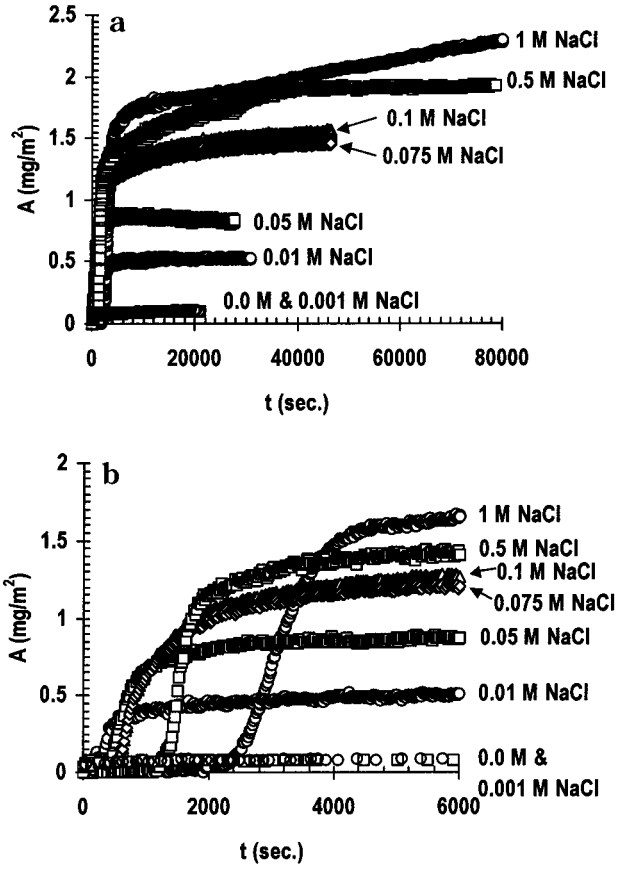

Figure 2. (a) Adsorbed amount A of hydrophobic−hydrophilic (electrolytic) diblock (PtBMA-*b*-PGMAS) on hydrophobic surface as a function of time t for various salt concentrations over a prolonged period of adsorption time. The PtBMA-*b*-PGMAS concentration was 100 ppm. (b) Adsorbed amount A of hydrophobic−hydrophilic (electrolytic) diblock (PtBMA-*b*-PGMAS) on a hydrophobic surface as a function of time t for various salt concentrations on a short time scale. The PtBMA-*b*-PGMAS concentration was 100 ppm.

shown in Figure 2a,b. After 12 h, there were only very little changes in ellipsometric angles under no added salt and under 0.001 M NaCl conditions.[33] When the salt concentration is raised to 0.01 M, a significant decrease in Δ and simultaneous increase in Ψ occurred after a certain period of time (~250 s), indicating the formation and subsequent growth of polymer layer. Therefore, one might suggest that the partial screening of hydrophilic block (PGMAS) facilitates the anchoring of molecules on the hydrophobized silicon wafers. The adsorbed polymer amount increases monotonically after the incubation period and reaches a plateau value at ca. 500 s, as shown in Figure 2a,b. The increase in salt concentration leads to an increase in the incubation time (Figure 3) and an increase in the equilibrium adsorbed amount (plateau value) (Figure 4). The increase in added salt concentration reduces the electrostatic interactions within and among chains, reducing the repulsions between adjacent hydrophilic blocks and therefore facilitating the adsorption on the substrate. The ellipsometric data obtained from the adsorption studies of PGMAS on the hydrophobic surfaces have shown no sign of adsorption in no added salt. These results suggest that the PGMAS does not adsorb on the hydrophobic surfaces under no added salt conditions. However, when the salt concentration is raised to 1 M, there is a little change in Ψ and Δ, which indicates weak adsorption of the PGMAS on the surfaces.[34] Figure 5

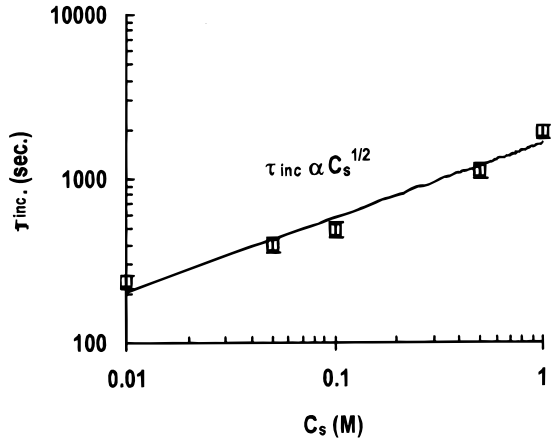

Figure 3. Incubation time τ_{inc} measured on hydrophobic surface as a function of NaCl concentration C_s. The incubation time scales with salt concentration with an exponent of $^1/_2$.

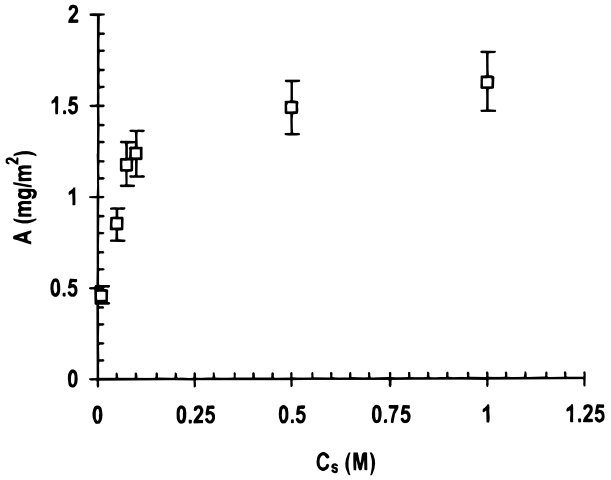

Figure 4. Plateau value of adsorbed amount A obtained for various salt concentrations on hydrophobic surface as a function of NaCl concentration C_s.

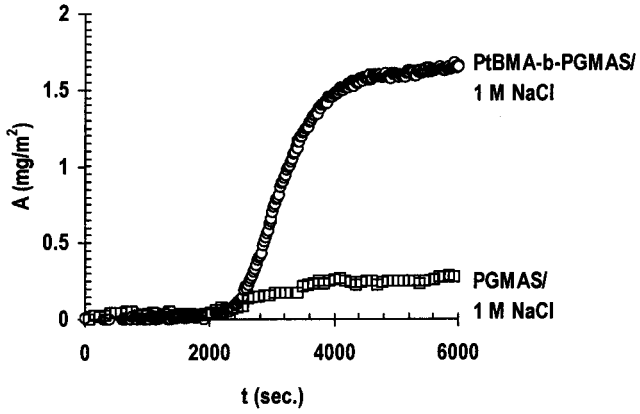

Figure 5. Adsorbed amount A of hydrophobic−hydrophilic (electrolytic) diblock (PtBMA-*b*-PGMAS) and homopolymer PGMAS on hydrophobic surface as a function of time t for 1 M NaCl salt concentration. Both PtBMA-*b*-PGMAS and PGMAS concentrations were 100 ppm.

shows the contrasts in adsorption behavior of PtBMA-*b*-PGMAS with that of PGMAS. The plateau value (corresponding to a quasi-equilibrium adsorption region) of adsorbed amount for PGMAS is found to be ca. 0.3 mg/m^2, which is considerably smaller than that of PtBMA-*b*-PGMAS obtained under similar added salt conditions. The adsorbed amount is ca. 5 times higher

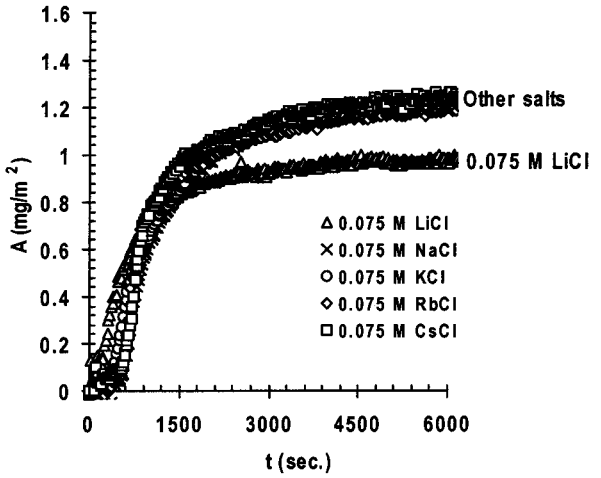

Figure 6. Adsorbed amount A of hydrophobic−hydrophilic (electrolytic) diblock (PtBMA-*b*-PGMAS) on hydrophobic surface as a function of time t for different counterion sizes. The PtBMA-*b*-PGMAS concentration was 100 ppm. Except for LiCl, the other salts, i.e., KCl, RbCl, and CsCl, do not make any resolvable difference in the adsorption characteristics with respect to NaCl.

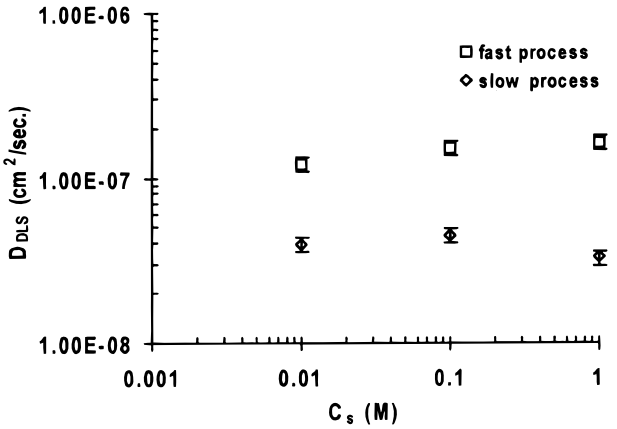

Figure 7. Diffusion coefficients in solution D_{DLS} as a function of NaCl concentration C_s. The fast process (D_f) and the diffusion coefficient for the slow process (D_s) do not change significantly within experimental errors as a function of the added salt concentration. The PtBMA-*b*-PGMAS concentration was 100 ppm.

for PtBMA-*b*-PGMAS compared to that for PGMAS. This suggests that the hydrophobic block plays a role in anchoring the block copolymer, and therefore it can be proposed that the adsorption process occurs through the anchoring of the hydrophobic chain on the hydrophobized substrate caused by the short-ranged hydrophobic interactions. Such adsorbed topology is quite reasonable as it minimizes the energetically unfavorable contact between the hydrophobic block and the aqueous solution and maximizes the favorable contact between hydrophilic block and aqueous medium.

Adsorption on Hydrophobic Surface. Effect of Added Monovalent Counterion Size. In this set of experiments, different counterions (Li^+, Na^+, K^+, Rb^+, and Cs^+) were investigated for a given salt concentration (0.075 M) in order to study the effects of counterion size on adsorption behavior. The results (Figure 6) show that, except for Li^+, all counterions do not make any resolvable difference in the adsorption characteristics. This means that the incubation period, the plateau adsorption value, and the rate of adsorption are the same as those measured with NaCl. In the case of LiCl, no incubation time was observed, and the equilibrium amount of adsorption is significantly less compared to that of other monovalent salts. The differences might arise from the degree of hydration or size of each counterion species. The bare ion radius of Li^+, Na^+, K^+, and Cs^+ is 0.068, 0.095, 0.133, and 0.169 nm, respectively.[35] However, the dimension we should consider is the hydrated radius. The hydrated radius and hydration number depend on how it is measured; the difference between the results obtained from different methods can be as much as 0.1 nm. Therefore, a relative or qualitative indicator is more adequate, and the reference framework should be the fact that smaller ions are more hydrated and tend to have a larger hydrated radius than larger ions. Thus, the order of hydration number is $Li^+ > Na^+ > K^+ > Rb^+ > Cs^+$. It is also known that hydration values are very much dependent on the salt concentration. At low salt concentration (0.1 M), the ionic hydration values appear to be $Li^+ = 62$ and $Na^+ = 44$ and much smaller at higher concentration.[36] Therefore, for the concentration studied (0.075 M), we can expect that the highly hydrated Li^+ ion is larger and hence less effective in the screening effect than the less hydrated Na^+ ion. On the other hand, contrary to the expectation, the counterions bigger than Na^+, i.e., K^+, Rb^+, and Cs^+, do not make any resolvable difference in the adsorption pattern from that of Na^+.

Diffusion of the PtBMA-*b*-PGMAS Solution at Various Added Salt Concentrations. The dynamic light scattering studies were performed at 120° with 100 ppm PtBMA-*b*-PGMAS solution under different added salt conditions. The data were analyzed using the CONTIN program which gives various relaxation processes (or diffusion processes), and the results are shown in Table 2. Two diffusion processes were observed: (i) a fast diffusion process which can be ascribed to individual molecules and (ii) a slow diffusion process which can be attributed to the motion of aggregates (micelles). The diffusion coefficient for the fast process (D_f) slightly increases with increasing salt concentrations, while the diffusion coefficient for the slow process (D_s) first slightly increases and then slightly decreases as a function of the added salt concentration (Figure 7). However, taking experimental errors into account (5−10%), no conclusion can be drawn on those small variations, and the diffusion coefficients can be considered to be essentially constant under the different salt concentrations studied.

Discussion

Comparing the adsorption data of PtBMA-*b*-PGMAS and PGMAS in 1 M NaCl solution, it can be ascertained that the anchoring of molecules takes place through the hydrophobic part of the PtBMA-*b*-PGMAS molecules since the adsorbed amount is found to be significantly small for PGMAS homopolymer. In general, kinetic data reveal three distinct stages in the PtBMA−NaPGMAS adsorption process: an incubation, a subsequent fast growth of adsorbed layer, and a plateau (equilibrium) region. As we have seen, these three stages depend on the salt concentration as well as counterion size.

The hydrophobic block is in a bad solvent and therefore can be assumed to adsorb on the hydrophobic surface in a collapsed state ($R_F = aN^{1/3}$), whereas the polyelectrolyte block carrying negative charge must be completely solvated and dangles in solution. A threshold

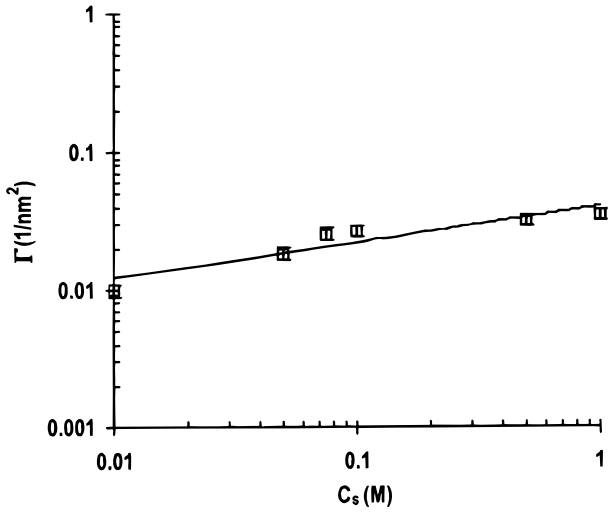

Figure 8. Surface density Γ obtained with hydrophobic surface as a function of salt concentration C_s. The surface density scales with salt concentration with the exponent of $^1/_4$.

Table 2. Dynamic Light Scattering Data

NaCl concn (M)	R_{H1} (nm)	R_{H2} (nm)	D_{fDLS} (cm²/s)	D_{sDLS} (cm²/s)
0.01	18.11	55.91	1.21×10^{-7}	3.93×10^{-8}
0.1	14.45	49.66	1.52×10^{-7}	4.42×10^{-8}
1.0	13.49	67.16	1.62×10^{-7}	3.27×10^{-8}

Table 3. Measured Adsorption Characteristics

NaCl concn (M)	A_p (mg/m²)	Γ (1/nm²)	d (nm)
0.01	0.46	0.009 98	10.01
0.05	0.85	0.018 44	7.36
0.075	1.18	0.025 61	6.25
0.1	1.24	0.026 91	6.10
0.5	1.49	0.032 33	5.56
1	1.63	0.035 37	5.32

salt concentration, i.e., 0.01 M NaCl, is needed for adsorption at a measurable level. As we could see, the equilibrium adsorbed amount (mg/m²) increases as a function of salt concentration due to the increase in sreeening of electrostatic interactions. One can obtain the grafting density, Γ, from the measured adsorbed amount, A (obtained by ellipsometry), using the following equation:

$$\Gamma\ (\text{number of chains/nm}^2) = \frac{A\ (\text{mg/m}^2) N_{av}\ (1/\text{mol})}{1000 M_w\ (\text{g/mol}) \times 10^{18}} \quad (6)$$

The interchain distance d is given by

$$d = \frac{1}{\sqrt{\Gamma}} \quad (7)$$

The results are shown in Table 3. The plot of Γ as a function of salt concentration (C_s) shows a power law dependence $\Gamma \propto C_s^{1/4}$ (Figure 8). The experimentally observed dependence appears to be much stronger than the power laws of mean field theoretical predictions[10] ($\Gamma \propto C_s^{1/11}$) and of scaling approach[3] ($\Gamma \propto C_s^{4/23}$) and much weaker than the theoretical prediction[3] for adsorption from the polymer solution above cmc ($\Gamma \propto C_s^{4/5}$).

Avrami Analysis. Let us explore the reasons for the existence of an incubation time. As shown in Figure 3, the incubation time τ_{inc} increases with salt concentration (C_s) according to a power law dependence:

$$\tau_{inc} \propto C_s^{1/2} \quad (8)$$

Many authors[37,38] have reported that the silanated surfaces have unreacted silanol groups (Si−OH) either from the substrate or from the silane agents. These unreacted silanol groups could interact with water or added salt.[39] The hydrophobized surfaces prepared for the experiments (see Materials) can very likely contain unreacted silanol groups. As described in the experimental part (see section on ellipsometry), initially the cell containing the hydrophobized substrate with the desired salt concentration solution was stabilized (ca. 1 h) before injecting a concentrated solution of PtBMA-*b*-PGMAS into the cell in order to get the final 100 ppm PtBMA-*b*-PGMAS solution. During the stabilization, the added counterions (Na^+) could interact with the unreacted silanol groups on the substrate and form a kind of bound ionic layer which changes the nature of the substrate on which the hydrophobic part of PtBMA-*b*-PGMAS chains adsorb. This bound ionic layer confined to the substrate may affect the direct interaction of the PtBMA blocks of the PtBMA-*b*-PGMAS diblock molecules with the substrate. Thus, the bound ionic layer would offer a barrier or resistance to the adsorption of hydrophobic part of the PtBMA-*b*-PGMAS diblock directly on the substrate, which is presumably responsible for the incubation time observed. As the salt concentration increases, the electrolytes compress the thickness of this ionic layer which results in the reduction of the Debye length (k^{-1}):[35]

$$k^{-1} \propto C_s^{-1/2} \quad (9)$$

Combining eqs 8 and 9, one can obtain the following relation:

$$k^{-1} \propto \frac{1}{\tau_{inc}} \quad (10)$$

Equation 10 suggests that as the confinement of counterions at the substrate increases (i.e., as Debye length decreases), the incubation time for the initiation of surface growth increases. Moreover, as the salt concentration increases, the sodium ions (Na^+) are less hydrated and hence smaller in size (in 0.1 M solution,[36] the ionic hydration value of Na^+ is 44 while in 1.0 M solution the hydration value of Na^+ is 8−9). These less hydrated sodium ions (Na^+) could move closer to the substrate than more hydrated ions. Therefore, the compressed ionic layer in conjunction with less hydrated sodium ions (Na^+) facilitates the formation of a stronger bound ionic layer that would in effect strengthen the barrier or resistance to the adsorption. Such a barrier or resistance would increase with increasing salt concentrations and would be more pronounced at higher salt concentrations. A threshold polymer concentration near the surface would be required to displace such a bound ionic layer and to initialize the surface growth process on the bare substrate. One may expect a higher threshold polymer concentration to displace the larger amount of bound simple ionic constituents from the substrate at higher salt concentrations. Such chain concentration buildup above the bound ionic layer

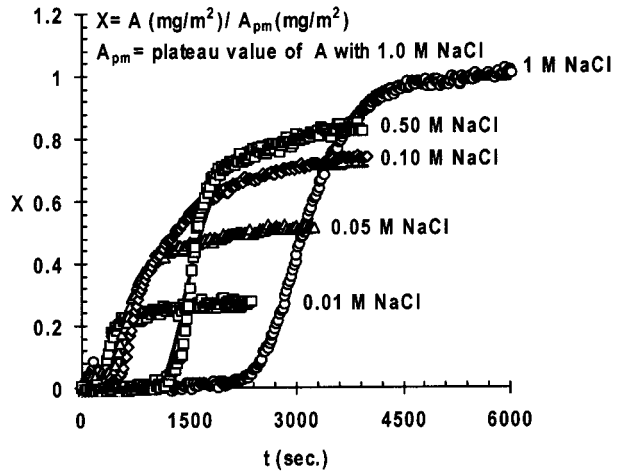

Figure 9. Normalized adsorbed amount X (i.e., the fraction of ordered polyelectrolyte phase on the hydrophobic substrate with respect to plateau value of A with 1 M NaCl) on hydrophobic surface as a function of time under different NaCl concentrations. The solid lines represent the fit with the Avrami equation (eq 11). The soild lines are not seen in most cases as the equation fits exactly with the data.

(confined to the substrate) may take a certain period of time, which would in fact increase the time for initiation of surface growth process with increasing salt concentration. Hence, we may attribute the bound ionic layer formation on the substrate to the incubation time. One may also speculate the reorientation of PtBMA-*b*-PGMAS (or PGMAS) molecules or their constituents (for example, dipoles) under different ionic strength conditions or the kinetic exchange of Na^+ ions between the OH groups on the substrate and the ionic sites as well as the OH groups of PtBMA-*b*-PGMAS molecules (see Figure 1) as alternate possible explanations for the increase of incubation time with added salt concentrations. We may add here, however, that with our experimental observations we are unable to make any solid judgment or attribute any specific reasons other than confinement of hydrated ions of added salt on the surface to the existence of incubation time or their functional dependency on added salt concentrations. A systematic investigation on the effects of temperature on adsorption characteristics for a given salt concentration, preferably with moderate salt concentrations (0.5 or 1.0 M), would reveal such kinetics and molecular details concerning incubation time.

Once the adsorption is initiated, the surface growth process is fairly fast, and within a short characteristic time the adsorption reaches an equilibrium value (plateau value). The growth process is very smooth, and the pattern of adsorption, i.e., surface growth process, looks very much similar to an Avrami type ordering process (phase change).[40−42] For the given sets of experiments of different salt concentrations ranging from 0.001 to 1.0 M NaCl with hydrophobic substrates, the maximal plateau adsorbed amount (A_{pm}) is observed with 1.0 M NaCl.[43] One could assume a well-ordered polyelectrolyte surface structure at 1.0 M NaCl and therefore normalize the measured adsorption density as a function of time (for the different added salt concentrations) with respect to the quantity A_{pm}. The resulting quantity, i.e., $X = A_i/A_{pm}$, gives the fraction of ordered polyelectrolyte phase on the substrate. The fractions X are plotted in Figure 9 as a function of time under different added salt concentrations. The plot thus

Table 4. Avrami Fit Parameters

NaCl concn (M)	0.01	0.05	0.1	0.5	1.0
τ (s)	219	424	642	673	1421
β	1.040	1.10	1.10	1.91	2.55

obtained can be analyzed with an Avrami type equation:[40−42]

$$X(t) = X_i + \Delta X\{1 - \exp[-(t/\tau)^{\beta}]\} \qquad (11)$$

where X_i signifies the initial ordered fraction before the onset of adsorption process ($t = 0$), ΔX is the change in ordered fraction during the ordering process, τ is the characteristic time constant, and β denotes the dimensionality of the surface growth. All the parameters expect β and τ can be obtained from the experimental data. By fitting eq 11 to the experimental data, one may obtain the Avrami exponent (β) and characteristic time (τ). The Avrami equation fits and the fitted Avrami parameters are shown in Figure 9 and Table 4, respectively. One could easily see that the fitted dimensionality (β) of the surface growth process increases with increasing salt concentrations. At high added salt concentrations, namely 0.5 and 1.0 M NaCl, the Avrami exponent (β) is nearly two. This result suggests that the PtBMA-*b*-PGMAS layers may grow on hydrophobic surface via isotropic two-dimensional growth mechanism with heterogeneous nucleation under the high screening regime. However, at low salt concentrations (from 0.01 M up to 0.1 M NaCl), the Avrami exponent (β) is nearly one. Therefore, one could presume an isotropic one-dimensional growth mechanism with heterogeneous nucleation of PtBMA-*b*-PGMAS layers on the surface. At higher salt concentrations, due to the higher degree of confinement of counterions (Na^+) on the surface, the incubation time is significantly higher than the one observed at low salt concentrations. At the same time, the higher salt solutions effectively screen the ionic sites of the hydrophilic part of PtBMA-*b*-PGMAS molecule, and this electrostatic screening process reduces the dimension of the individual chains as evident from the DLS measurements (Figure 7).

As we have discussed above, at high added salt conditions a high threshold polymer chain concentration is required near the surface to displace the larger amount of bound simple ionic constituents from the substrate and to initialize growth process on the bare substrate. One might anticipate a higher order growth process under such conditions due to the higher chain concentrations near the surface. Thus, one could justify higher order growth under higher salt concentrations. At low salt concentrations ranging from 10 to 100 mM NaCl, since the degree of ion binding to the substrate is less, the barrier to the initiation of adsorption process is considerably low, and therefore the incubation time is small. At the same time, the partial screening could reduce electrostatic interactions within and between the chains so that these species can approach each other closer than without added salt conditions and adsorb on the substrate. Since the polymer chains are still partially charged and the incubation time for the onset of adsorption is low (therefore the chain concentration near surface is also low), one could anticipate a one-dimensional surface growth process in this case. Thus, the fitted parameter β (the dimensionality of the growth process) is justified. In general, we may conclude that the buildup of polyelectrolyte layer structure very much depends on added salt conditions.

Our adsorption kinetic data are qualitatively very different from the two-stage process models, i.e., initial diffusion limited regime and subsequent brush limited regime, which are conventionally used to describe diblock copolymers (including diblock polyelectrolyte) adsorptions.[21,28] As already discussed before, the nucleation and growth of the adsorbed layer seem to be the determining processes as it has been described in the Avrami model. However, the Avrami model gives only a phenomenological description of the adsorption kinetics without revealing much information about molecular details. Thus, there might be real patches of adsorbed chains formed in the initial stage of adsorption, which then grow in size with time.

Conclusions

We have investigated the adsorption kinetics of a diblock copolymer poly(*tert*-butyl methacrylate)−sodium poly(glycidyl methacrylate sulfonate) on hydrophobic substrate from aqueous solution under different added monovalent salt (NaCl) concentrations using ellipsometric technique. The effect of monovalent counterion size on adsorption kinetics of the same copolymer on hydrophobic surface has also been a part of the investigation. When we compare the adsorption data of both PtBMA-*b*-PGMAS and PGMAS on hydrophobic substrate, it is clear that the anchoring of molecules takes place through hydrophobic part of the PtBMA-*b*-PGMAS molecules. In general, the kinetic data reveal three distinct stages of the adsorption process: an incubation, a subsequent fast growth of polymer layer, and an equilibrium region. The three stages are found to be dependent on the salt concentrations as well as on the counterion size. The equilibrium adsorbed amount increases as a function of salt concentration due to the increase in the electrostatic screening effect. The plot of adsorption density (Γ) as a function of salt concentration shows a power law dependence, $\Gamma \propto C_s^{1/4}$, which is stronger than the power laws of both mean field and scaling approaches for adsorption from aqueous dilute solution below the cmc. The dependence, though, is much weaker than the theoretical prediction for adsorption from the polymer solution above the cmc.

In contrast to the currently available experimental information for closely similar systems, an incubation period for initiation of adsorption is observed. The incubation time increases with salt concentration according to a power law dependence. We propose a bound ionic layer formation on the substrate as a possible reason for the incubation time. However, the authors do not rule out other possibilities such as reorientation of PtBMA-*b*-PGMAS molecules or their constituents (for example, dipoles) under different ionic strength or the kinetic exchange of Na^+ ions between the OH groups on the substrate, etc. An attempt has been made to explain the growth process and the pattern of adsorption, i.e., the slow birth (nucleation) and fast growth process in terms of an Avrami type ordering process. The analysis suggests that a slow nucleation and subsequent fast growth of the layer during adsorption seems to be the determining process. The Avrami analysis also suggests that the buildup of polyelectrolyte layer structure is very much dependent on added salt conditions.

As an extension to this work it would be interesting to probe the effects of temperature on adsorption characteristics for a given salt concentration, preferably with moderate salt concentrations (0.5 or 1.0 M) which may reveal more kinetic and molecular details concerning incubation time and the dissolution process of micelles, etc. Also, it would be interesting to take atomic force microscope (AFM) images of lateral structures at different stages of adsorption, preferably with moderate salt concentrations (0.5 or 1.0 M) as an effort to corroborate the observed growth kinetics and the evolution of aggregate structures.

Acknowledgment. We appreciate the help of H. Walter concerning the ellipsometric measurements and S. Wiegand concerning the light scattering measurements. T.A. is grateful to the Max-Planck-Institut für Polymerforschung for the hospitality during the ellipsometric measurements. This work was financially supported by funds from the Natural Sciences and Engineering Research Council of Canada (NSERC) and the Fonds pour la Formation de Chercheurs et l'Aide de la Recherche du Québec (FCAR). Also, J. F. Gohy and R. Jérôme are very much indebted to the Services Fédéraux des Affaires Scientifiques, Techniques et Culturelles for financial support in the frame of the Pôles d'attraction Interuniversitaires: 4-11: Chimie et Catalyse Supramoléculaire.

References and Notes

(1) Barret, J. L.; Joanny, J.-F. *Adv. Chem. Phys.* **1996**, *94*, 1−66.
(2) Föster, S.; Schmidt, M. *Adv. Polym. Sci.* **1995**, *120*, 50−133.
(3) Dan, N.; Tirrell, M. *Macromolecules* **1993**, *26*, 4310−4315.
(4) Wittmer, J.; Joanny, J. F. *Macromolecules* **1993**, *26*, 2691−2697.
(5) Marko, J.; F.; Rabin, Y. *Macromolecules* **1992**, *25*, 1503−1509.
(6) Moffitt, M.; Khougaz, K.; Eisenberg, A. *Acc. Chem. Res.* **1996**, *29*, 95−102.
(7) Guenoun, P.; Davis, H. T.; Tirrell, M.; Mays, J. W. *Macromolecules* **1996**, *29*, 3965−3969.
(8) Guenoun, P.; Delsanti, M.; Gazeau, D.; Mays, J. W.; Cook, D. C.; Tirrell, M.; Auvary, L. *Eur. Phys. J. B.* **1998**, *1*, 77−86.
(9) Astafieva, I.; Zhong, X. F.; Eisenberg, A. *Macromolecules* **1993**, *26*, 7339−7352.
(10) Argilliar, J. F.; Tirrell, M. *Theor. Chim. Acta* **1992**, *82*, 343−350.
(11) Hariharan, R.; Biver, C.; Russel, W. B. *Macromolecules* **1998**, *31*, 7514.
(12) Misra, S.; Tirrell, M.; Mattice, W. *Macromolecules* **1996**, *29*, 6056−6060.
(13) Pincus, P. *Macromolecules* **1991**, *24*, 2912−2919.
(14) Ross, R. S.; Pincus, P. *Macromolecules* **1992**, *25*, 2177−2183.
(15) Zhulina, E. B.; Borisov, O. V. *J. Chem. Phys.* **1997**, *107*, 5952−5969.
(16) Miklavic, S. J.; Marcelja, S. *Macromolecules* **1988**, *21*, 6718−6722.
(17) Borisov, O. V.; Zhulina, E. B. *Eur. Phys. J. B* **1998**, *4*, 205−217.
(18) Borisov, O. V.; Zhulina, E. B. *J. Phys. II* **1997**, *7*, 449−458.
(19) Borisov, O. V.; Birshtein, T. M.; Zhulina, E. B. *J. Phys. II* **1991**, *1*, 521−526.
(20) Borisov, O. V.; Zhulina, E. B.; Birshtein, T. M. *Macromolecules* **1994**, *27*, 4795−4803.
(21) Motschmann, H.; Stamm, M.; Toprakcioglu, Ch. *Macromolecules* **1991**, *24*, 3681−3688.
(22) Dorgan, J. R.; Stamm, M.; Toprakcioglu, C.; Jerome, R.; Fetters, L. J. *Macromolecules* **1993**, *26*, 5321−5330.
(23) Siqueira, D. F.; Stamm, M.; Breiner, U.; Stadler, R. *Polymer* **1995**, *36*, 3229−3233.
(24) Halperin, A.; Tirrell, M.; Lodge, T. P. *Adv. Polym. Sci.* **100**, 31−71.
(25) Munch, M. R.; Gast, A. P. *Macromolecules* **1990**, *23*, 5313.
(26) Filippova, N. L. *Langmuir* **1998**, *14*, 1162−1176 and references therein.
(27) Shubin, V.; Linse, P. *J. Phys. Chem.* **1995**, *99*, 1285−1292.
(28) Amiel, C.; Sikka, M.; Schneider, J. W., Jr.; Taso, Y. H.; Tirrell, M.; Mays, J. W. *Macromolecules* **1995**, *28*, 3125−3134.

(29) Walter, H.; Harrats, C.; Muller, P.; Jerome, R.; Stamm, M. *Langmuir* **1999**, *15*, 1260−1267.
(30) Hüttenbach, S.; Stamm, M.; Reiter, G.; Foster, M. *Langmuir* **1991**, *7*, 2438−2442.
(31) Azzam, R. M. A.; Bashara, N. M. *Ellipsometry and Polarized Light*; North-Holland Publication: Amsterdam, 1987.
(32) De Feitjer, J. A.; Benjamins, J.; Veer, F. A. *Biopolymers* **1978**, *17*, 1759.
(33) There is very little change in ellipsometric angles with no added and 0.001 M NaCl, and the corresponding adsorbed amount is found to be ≤ 0.1 mg/m^2 (obtained when the measured values are averaged over four points). Scatter in data is too high to judge the pattern of adsorption. The adsorbed amount may be very small to be detected by ellipsometry method due to the sparse tethering of diblock polyelectrolyte on the substrate. Since the adsorbed amount values are very little and the initial adsorption region hard to identify, the data are not considered in further kinetic analysis.
(34) Scatter in data was quite remarkable. Therefore, the measured values are averaged over four points.
(35) Israelachuili, J. N. *Intermolecular & Surface Forces*, 2nd ed.; Academic Press: London, 1992.
(36) Glasstone, S. *Electrochemistry of Solutions*; D. Van Nostrand Company: New York, 1967; Chapter 3, pp 45−54.
(37) Le Grange, J. D.; Markham, J. L.; Kurkjian, C. R. *Langmuir* **1993**, *9*, 1749−1753.
(38) Wasserman, S. R.; Whiteside, G. M.; Tidswell, I. M.; Ocko, B. M.; Pershan, P. S.; Axe J. D. *J. Am. Chem. Soc.* **1989**, *111*, 5852−5860.
(39) Iler, R. K. *The Chemistry of Silica*; John Wiely & Sons: New York, 1979; Chapter 6. Iler, R. K. *The Chemistry of Silica*; John Wiely & Sons: New York, 1979; Chapter 6.
(40) Avrami, M. *J. Chem. Phys.* **1939**, *7*, 1103−1112.
(41) Avrami, M. *J. Chem. Phys.* **1939**, *8*, 212−224.
(42) Avrami, M. *J. Chem. Phys.* **1939**, *9*, 117−184.
(43) We were unable to perform experiments with higher salt concentrations than 1.0 M as the ellipsometric angle measurements are frequently obstructed by bubble formation on the glass window.

MA991207J